Lymphoid neogenesis in chronic rejection: Evidence for a local humoral alloimmune response

Olivier Thaunat*†, Anne-Christine Field*, Jianping Dai‡, Liliane Louedec‡, Natacha Patey§, Marie-Françoise Bloch*, Chantal Mandet*, Marie-France Belair*, Patrick Bruneval*, Olivier Meilhac‡, Blanche Bellon*, Etienne Joly¶, Jean-Baptiste Michel‡‖, and Antonino Nicoletti*‖

*Institut National de la Santé et de la Recherche Médicale U681, Institut Biomédical des Cordeliers, Université Pierre et Marie Curie Paris VI 75006 Paris, France; ‡Institut National de la Santé et de la Recherche Médicale U698, Hôpital Xavier Bichat, 75870 Paris, France; §Department of Pathology, Hôpital Necker, 75270 Paris, France; and ¶Institut National de la Santé et de la Recherche Médicale U563, L'Institut Fédératif de Recherche Claude de Preval, 31300 Toulouse, France

Communicated by Jean Dausset, Fondation Jean Dausset, Centre d'Etude du Polymorphisme Humain, Paris, France, August 29, 2005 (received for review June 10, 2005)

Recent advances indicate that, in various chronic inflammatory disorders, the activation of the immune system is triggered locally rather than in lymphoid organs. In this study, we have evaluated whether the humoral alloimmune response involved in chronic rejection is elicited within the graft. We used the rat aortic interposition model and microdissected the adventitia of the graft. Over time, the T cell infiltrate shifted toward a B helper phenotype. B lymphocyte clusters were detected and were the site of intense proliferation and apoptosis. Simultaneously, adventitial vascular endothelium acquired a high endothelial venule phenotype. Similar features were evidenced in the interstitium of chronically allografts (hearts and kidneys). Strikingly, ganocultured graft interstitial tissue was found to be the site of production of antibodies directed against donor MHC-I molecules. These findings, therefore, document the appearance of germinal centers in chronically rejected tissues. This lymphoid neogenesis implies that the graft is not only the target of the alloimmune response but also a site where this response actually develops, so as to optimize the communication between the targeted tissue and the immune effectors.

chronic rejection | transplantation | B cells | germinal centers | adventitia

Despite recent advances in transplantation, the long-term outcome of transplanted organs remains impeded by chronic rejection (1). Accumulating evidence suggests that humoral immunity (2–4) and, particularly, alloantibodies directed against donor MHC I molecules (5–8) are critical in the pathogenesis of chronic vascular rejection.

Clinically, chronic rejection is responsible for a slow deterioration of graft function, which correlates with typical histological changes. Excluding organ-specific manifestations, the most common histopathological feature is chronic vascular rejection, also known as allograft arteriosclerosis, characterized by widespread and diffuse narrowing of the vascular lumen as a result of intimal proliferation of smooth muscle cells and fibroblasts and destruction of smooth muscle cells from the media (9–12). Chronic vascular rejection is also typified by an abundant adventitial inflammatory infiltrate (9). We therefore evaluated whether the humoral alloimmune response was elicited within the adventitia of the graft. In such case, chronic vascular rejection would be similar to other chronic inflammatory disorders in which tissue destruction results from a vicious circle maintained by an uncontrolled local immune response.

We demonstrate the involvement of intragraft lymphoid neogenesis in the development of chronic rejection in an animal model, based on aortic transplantation between histoincompatible strains of rats (13–16). We show that the adventitial inflammatory infiltrate harbors a secondary lymphoid organ structure and that anti-donor MHC I antibodies are produced within these structures. Additionally, we provide insights into the clinical relevance of these observations because similar lymphoid structures were detected in the interstitium of human chronically rejected grafts.

Materials and Methods

Animals. Age-matched male Brown-Norway (BN; $RT1^n$) and Lewis rats (LEW; $RT1^l$) were obtained from Charles River Breeding Laboratories. LEW rats were used as recipients and syngeneic donors and BN rats were used as allogeneic donors. All animal experimentation was undertaken in compliance with the European Community standards (authorization no. 75-214). Animals were kept under conventional conditions and fed a standard diet.

Aorta Transplantation. Rats were anesthetized with 50 mg/kg pentobarbital injected i.p. Two animals were operated simultaneously, one as the donor of aortic graft and the other as the recipient, with the aid of an operating microscope. A 1-cm-long segment of the donor abdominal aorta was excised, perfused with normal saline, and small collateral arteries that originated from the graft were ligated. The donor aorta was transplanted in orthotopic position by end-to-end anastomosis in the recipient aorta below the renal arteries and above the iliac bifurcation. We used the 94 of 100 animals that survived to the surgical procedure. No immunosuppressive or anticoagulant treatment was used. At 10 days, 1 month, and 2 months posttransplantation, aortic grafts were removed from the Lewis recipients under anesthesia and perfused with saline. These three time points were selected in accordance with one of our previous studies (17), which showed that they correspond, respectively, to three successive stages of the rejection process. Indeed, the cellular cytotoxic response takes place 10 days posttransplantation, followed by the humoral response and scarring process, respectively, 1 and 2 months posttransplantation.

Fresh aortic samples were dissected and embedded in paraffin or snap frozen immediately in optimal cutting temperature (OCT) medium (Tissue-Tek, Agar Scientific, Stansted, Essex, U.K.) in liquid nitrogen.

Isolation of Adventitial Cells. Cells within the adventitia of the graft were isolated as described in ref. 18 by microdissection, digestion in a collagenase I solution (GIBCO/Invitrogen), and filtration through 100-μm nylon meshes.

Antibodies. The following mouse anti-rat mAbs (Serotec) were used: anti-TCR$\alpha\beta$ (R73; T cells), anti-CD4 (OX35; helper T cells), anti-CD8α (OX8; cytotoxic T cells), anti-CD134 (OX40), anti-RT1-B (OX6; MHC II molecule), and anti-ED1 (macrophages). In addition, anti-CD25 (OX39; RIL-2 receptor α chain), anti-IFNγ antibodies, and adequate murine isotypic controls were used (BD

Abbreviations: HEV, high endothelial venule; PCNA, proliferating cell nuclear antigen.

†To whom correspondence should be addressed at: Institut National de la Santé et de la Recherche Médicale U681, Institut des Cordeliers, 15 Rue de l'Ecole de Médecine, 75006 Paris, France. E-mail: olivier.thaunatpastu@free.fr.

‖J.-B.M. and A.N. contributed equally to this work.

Pharmingen). B lymphocytes were detected with anti-rat Ig κ chain antibodies (MARK 1, Lo-Imex, Brussels) for flow cytometry and with anti-pan B cell antibodies (RLN-9D3; Serotec) for immunohistology. Heavy-chain isotypes of surface immunoglobulins on B lymphocytes were defined with anti-δ (MARD-3) and anti-μ (MARM-4) antibodies (Lo-Imex).

Immunohistological Analysis. Cryosections were air dried and fixed in acetone. Endogenous biotin and avidin were blocked (Biotin–Avidin Block, DAKO). We used a biotin-conjugated horse anti-mouse secondary antibody (Vector Laboratories). Immunohistochemical staining was revealed by using alkaline phosphatase anti-alkaline phosphatase complexes. Alkaline phosphatase was detected by incubation with a revelation substrate (fast red salt dissolved in Tris buffer containing naphthol and levamisole) prepared just before use. Sections were counterstained with hematoxylin.

Flow Cytometry. ***Detection of cell-surface antigens.*** Cells (0.1 million) were stained with FITC-, phycoerythrin (PE)-, or biotin-conjugated mAbs. Biotinylated mAbs were revealed with streptavidin-PE (BD Biosciences). After washing, cells were fixed in PBS containing 1% of formaldehyde. Fluorescence was detected by using a FACScan and analyzed by using the program CELLQUEST (BD Biosciences). Cells were counted in a tight electronic gate set on the lymphocyte cluster on the forward and side scatter plot.

Detection of intracellular IFNγ. Measurement of IFNγ production was performed by combined surface and intracellular staining with mAbs and subsequent three-color flow cytometric analysis. Adventitial lymphocytes were stimulated with phorbol 12-myristate 13-acetate (50 ng/ml; Sigma-Aldrich) and ionomycin (1 μg/ml; Calbiochem) for 6 h and cytokine secretion inhibited by treatment with 10 μg/ml brefeldin A (Alexis, Lausanne, Switzerland) the last 2 h of incubation. Stimulated cells were washed and stained with FITC-conjugated anti-TCR$\alpha\beta$ antibodies and with CyChrome-conjugated anti-CD4 or PerCP-conjugated anti-CD8α antibodies. Double-labeled cells were fixed and permeabilized with a 0.1% saponin solution (Sigma-Aldrich). Intracellular staining was performed with a PE-conjugated anti-rat IFNγ antibody. Cells were washed twice in a 0.1% saponin solution and resuspended in PBS for flow cytometry analysis. Cells were counted in a tight electronic gate set on the lymphocyte cluster on the forward and side scatter plot. $CD4^+$ and $CD8^+$ cells expressing IFNγ were counted among TCR$\alpha\beta$-positive cells.

Apoptosis. The TUNEL technique (19) was used to detect apoptosis. *In situ* 3-end labeling of apoptotic DNA was performed by using Apotag Peroxidase kits (Oncor) on paraffin-embedded sections, following the manufacturer's instructions. Briefly, after dewaxing, rehydration, and blocking of endogenous peroxidase, 3-hydroxy-DNA strand breaks in permeabilized tissue sections were enzymatically labeled with digoxigenin-nucleotides, by using terminal deoxynucleotidyl transferase. The labeled DNA was then bound with antidigoxigenin antibody peroxidase conjugate, and the peroxidase color reaction was developed with a 3-amino-9-ethyl carbazole substrate.

Proliferation. Cell proliferation was assessed by immunohistochemistry of proliferating cell nuclear antigen (PCNA) as described in ref. 20. The monoclonal Ab PC 10 (Dakopatts) was applied to paraffin-embedded sections after antigen retrieval in a microwave oven for 5 min in 0.1 M EDTA buffer (pH 8.0).

Transmission Electron Microscopy. Electron microscopy analysis was performed on aortic grafts 10 days (10 grafts) and 2 months (5 grafts) after transplantation. Aortic graft specimens were harvested, immediately fixed in 2.5% glutaraldehyde in PBS buffer, postfixed in 4% osmium tetroxide, and embedded in Epon resin. Semithin sections (1–2 μm thick) were used to locate vascular tissue in the adventitia of the graft. Ultrathin sections (50–80 nm thick) were prepared, stained with lead citrate and uranyl acetate, and observed with a Zeiss EMI transmission electron microscope. Temporal changes in the morphology of endothelial cells of graft adventitial arterioles, venules, and capillaries were tracked.

In Vitro* Production and Characterization of Alloantibodies.** ***Organoculture. Microdissected adventitia of aortic grafts and untouched thoracic aortas, draining lymph nodes, and spleens were recovered from 20 Lewis recipients 1 month posttransplantation and placed in cold sterile X-VIVO 15 serum-free medium (Cambrex, Walkersville, MD) with 100 units/ml penicillin/streptomycin and 25 μg/ml Fungizone (GIBCO). Tissues were washed three times in fresh medium. Each sample was fragmented with a sterile razor blade, placed into 2 ml of fresh medium, and cultured in 24-well plates at 37°C under hyperoxic conditions (80% O_2/20% CO_2). Culture supernatants were recovered after 4 days of culture.

Specificity of locally produced antibodies. The analysis of the specificity of the antibodies present in the organoculture-derived supernatants was performed by flow cytometry by using Lewis (recipient) fibroblasts expressing or not expressing Brown-Norway (donor) MHC I molecules. These cells were obtained as follows. The cDNA for RT1-$A1^n$ (nucleotide sequence from the EMBL database, accession no. X90375.1) was cloned in the BamH1 site of the pLXLJ vector and transfected into Ψ 2 cells as described in refs. 21 and 22. Culture supernatants from the G418-resistant Ψ 2 cells were used to infect Lewis fibroblasts (LEW-F). LEW-F cells expressing stable levels of functional RT1-$A1^n$ molecules were selected with G418 (GIBCO) at 0.5 mg/ml. All transfected LEW-F cells (LEW-F+$A1^n$) expressed RT1-$A1^n$ as assessed by flow cytometry using the OX27 monoclonal antibody [mouse anti-rat MHC I, specific for RT1-$A1^n$ (23), data not shown]. Appropriate isotypic controls were used (BD Biosciences).

One hundred microliters of each organoculture-derived supernatant were incubated with 200,000 LEW-F or LEW-F+$A1^n$ cells for 30 min at 4°C. The binding of antibodies on the cell surface was then determined with an anti-rat Ig κ light-chain FITC-conjugated antibody (MARK 1), by measuring the mean fluorescence intensity in a FACScan flow cytometer.

Processing of Human Tissues. ***Patients.*** Human tissue samples were obtained from patients during their follow-up at Necker Hospital. Five heart grafts were obtained from pediatric recipients (three males and two females, all Caucasians, with a mean age of 9.4 $\pm$ 0.7 years). These heart grafts were harvested at the time of retransplantation (mean transplantation period of 6.4 $\pm$ 3.6 years) required because of terminal chronic rejection inducing graft failure. Fifteen kidney grafts were obtained from adult recipients (nine males and six females, all Caucasians, with a mean age of 41.7 $\pm$ 3.8 years). These patients underwent transplant nephrectomy after return to hemodialysis because of kidney graft failure. In 10 patients, indication for graft removal was terminal chronic rejection after a mean transplantation period of 8.7 $\pm$ 5.6 years. For the 5 remaining patients, transplant nephrectomy was performed after a transplantation period of $<$3 months because of primary graft failure (two graft arterial thrombosis, two graft vein thrombosis, and one ureteral necrosis). Five additional kidneys were removed for renal cancer (three males and two females, all Caucasians, mean age 50.7 $\pm$ 6.4 years). Five to 24 samples from each organ were studied by hematoxylin–eosin on paraffin sections to localize inflammatory cells. The reference number of inflammatory cells in a kidney was set as compared with the number found in the tissues away from the tumor.

Immunofluorescence. Indirect immunohistochemical stainings were performed by using a streptavidin–biotin complex method (24). Serial sections were deparaffinized and rehydrated. Endogenous peroxidase activity was blocked by methanol/H_2O_2. Tissue sections

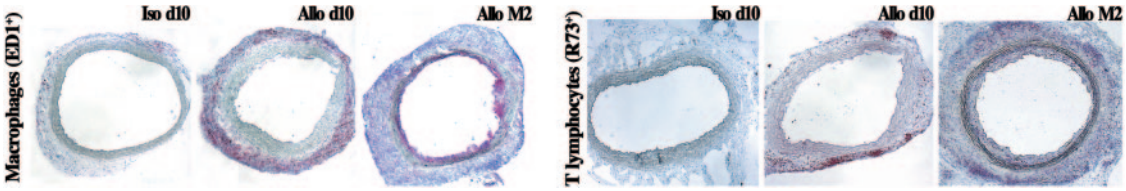

Fig. 1. Kinetics of immunodetection of adventitial mononuclear cells. Seven-micrometer-thick transversal sections of aortic isografts (*Left*) and allografts (*Center* and *Right*) harvested 10 days (d10) and 2 months (M2) posttransplantation and stained by using the alkaline phosphatase anti-alkaline phosphatase technique (original magnification, ×5). Primary monoclonal antibodies used were anti-macrophage (ED1) and anti-$\alpha\beta$TCR (R73). Note that 2 months posttransplantation (*Right*), adventitial infiltrate decreased in allografts, when all medial smooth muscle cells are destroyed, as assessed by media thinning. Development of neointima is detected at this time point.

underwent heat-induced antigen retrieval (25) with citrate buffer (15 min at 100°C). The following mouse anti-human antibodies (DAKO) were used: anti-CD20 (L26; anti-pan B cells), anti-CD3 (polyclonal; anti-pan T cells), anti-CD23 (MHM6; anti-follicular dendritic cells), and anti-Ki67 (MiB1; proliferation marker). The primary antibodies were applied to the sections by using dilution predetermined for optimal staining, followed by incubation with biotin-conjugated goat anti-mouse antibodies and streptavidin–biotin horseradish peroxidase complex (SABC/HRP; DAKO). Peroxidase activity was revealed by 3-amino-9-ethyl carbazole. The sections were counterstained with hematoxylin.

Statistical Analysis. Data were analyzed by using the program STATVIEW 5.0 (Abacus Concepts, Berkeley, CA). The statistical significance of the results was determined by one-way ANOVA followed by Fischer's probable least square difference tests. *P* values of <0.05 were considered as statistically significant.

Results

Kinetics of Aortic Allograft Adventitial Inflammatory Infiltration. Lewis rats were transplanted with Brown-Norway abdominal aortas and were killed at 10 days, 1 month, and 2 months posttransplantation. Grafts were harvested at each time point for analysis of their microanatomy and cellular composition. Aortic allografts presented a time-dependent leukocyte adventitial infiltration (Fig. 1). This infiltrate was mainly constituted of lymphocytes and ED1-positive macrophages. Most of the T cells infiltrated in the graft were located in the adventitial layer. The infiltrate increased between 10 days and 1 month posttransplantation, and T cells accumulated as a massive circumferential ring with external nodular reinforcements (Fig. 1). These nodules were enriched in $CD4^+$ T lymphocytes, whereas $CD8^+$ T lymphocytes had a more diffuse distribution (data not shown). The number of macrophages and T cells decreased at 2 months, leaving an acellular fibrous scar. By this time, medial smooth-muscle cells had disappeared from the graft (Fig. 1). Conversely, control isografts were devoid of leukocyte infiltration, but for a few scattered ED1-positive macrophages transiently present in the adventitia at day 10 (Fig. 1), which likely participate in surgical wound healing. These observations were corroborated by flow cytometry quantitative analysis on cell suspensions obtained after microdissection and enzymatic digestion of the graft adventitial layer (data not shown).

Adventitial Vascular Endothelium Acquires a High Endothelial Venule (HEV) Phenotype. Because we did not detect inflammatory cells across the medial layer, it seemed likely that the recruitment of leukocytes in the adventitia could be due to modifications of the permeability of the vasa-vasorum endothelium. Changes in the phenotype of endothelial cells in the adventitia of aortic grafts were, therefore, sought by electron microscopy. Ten days after transplantation, endothelial cells in certain venules, but not in arterioles, had acquired a HEV-like phenotype (Fig. 2*A*). These endothelial cells were plump, with large quantities of cytoplasm, and had an increased organelle content. The nuclei were ovoid with variable degrees of folding and widely dispersed granular heterochromatin. The luminal surface displayed numerous microvillous projections and protruded into the vessel lumen, creating intercellular clefts (Fig. 2*B*). Remarkably, these HEVs were detected exclusively in adventitial areas containing lymphocyte nodules (Fig. 2*A*). Non-inflammatory areas of the adventitia displayed venules with normal flat endothelial cells (Fig. 2*C*). Two months posttransplantation, adventitial inflammatory infiltrates were found to have resorbed and adventitial venular endothelial cells had resumed a normal phenotype (data not shown). These observations suggest that the acquisition of a HEV phenotype by venular endothelial cells in the adventitia is temporally and spatially correlated with the inflammatory infiltrate.

T Cell Infiltrates Acquire the Capacity to Help B Cells. Adventitial T cell infiltrates examined by flow cytometry 10 days posttransplantation were composed of ≈50% of $CD4^+$ T cells and ≈50% of $CD8^+$ T cells. The proportion of $CD4^+$ T cells as compared with $CD8^+$ T cells increased at 1 month (Fig. 3*A*). Concomitantly, the percentage of cells expressing the MHC II (RT1.B) and CD134 molecules increased among $CD4^+$ but not among $CD8^+$ T cells (Fig. 3 *C* and *D*), whereas both $CD4^+$ and $CD8^+$ T cells lost their capacity to secrete IFNγ (Fig. 3*D*). Taken together, these data point to a shift in the immune response. Down-regulation of the initial cellular cytotoxic alloimmune response was associated with the emergence of $CD4^+$ T cells that may display the capacity to help B cells to mature.

B Cells Infiltrate the Adventitia. Simultaneously with the changes in the adventitial T lymphocyte population, the proportion of B cells increased progressively among leukocytes recovered from the adventitial layer of aortic allografts and analyzed by FACS: B cells represented 12.75 ± 3.37% of the infiltrated leukocytes at 10 days and 23.94 ± 3.74% at 1 month ($P < 0.05$). Immunohistochemical analysis on longitudinal sections of aortic allografts also revealed

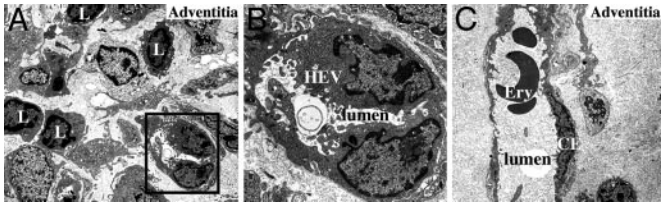

Fig. 2. Adventitia acquires HEVs. (*A–C*) Electron microscopy analysis of endothelial cells located in the adventitia of aortic grafts 10 days after transplantation (L, lymphocyte; Ery, erythrocyte; CE, normal flat venular endothelial cell). At 10 days posttransplantation, venular endothelial cells located nearby adventitial lymphocyte infiltrates displayed a HEV-like phenotype. (*A*) Original magnification, ×2,500. (*B*) Original magnification, ×8,000. (*C*) Normal flat venular endothelial cells were observed in quiescent areas of the adventitia at the same time point (original magnification ×2,500).

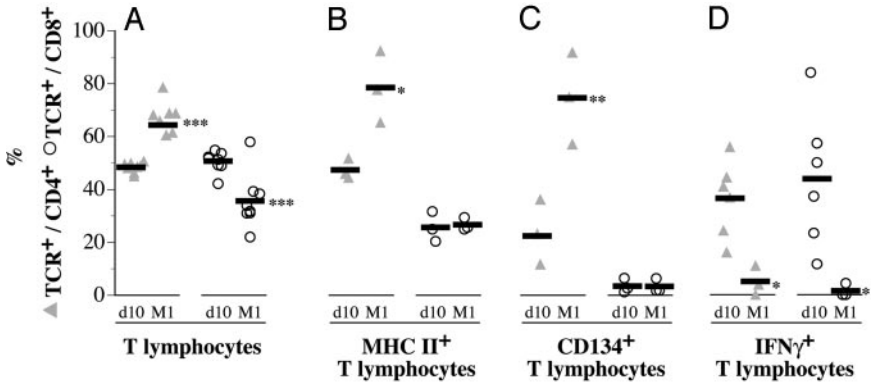

Fig. 3. Change in the phenotype of the T cell adventitial infiltrate. Adventitia of the allograft was selectively isolated by microdissection 10 days (d10) and 1 month (M1) posttransplantation. After digestion in a collagenase I solution, adventitial cells were suspended and analyzed by flow cytometry. (*A*) The lymphocyte composition in the adventitial infiltrate was evaluated by using anti-$\alpha\beta$TCR (R73), anti-CD4 (OX35), and anti-CD8 (OX8) mAbs. (*B*) Anti-MHC II (RT1.B) mAb was used to study the level of activation of the adventitial $CD4^+$ and $CD8^+$ lymphocyte subpopulations. (*C*) Anti-CD134 mAb was used to identify cells able to provide help to B cells among adventitial $CD4^+$ and $CD8^+$ lymphocyte subpopulations. (*D*) The evolution of the polarization of the adventitial T cell infiltrate was followed by measuring the percentage of IFNγ-producing lymphocytes by using combined surface and intracellular staining with anti-$\alpha\beta$TCR (R73), anti-CD4 (OX35), anti-CD8 (OX8), and anti-IFNγ mAbs. *, $P < 0.05$; **, $P < 0.01$; ***, $P < 0.001$; d10 vs. M1; each symbol represents an animal, and the bold line represents the mean value.

the presence of B cells, exclusively in the adventitial layer (Fig. 4). These cells were clustered in nodular aggregates located in the outer part of the graft adventitia and were surrounded by a ring of T cells. We also noted that B cell clusters were larger at 1 month than on day 10 (data not shown).

The Adventitial Inflammatory Infiltrate Is Structured as a Secondary Lymphoid Tissue. To characterize the B cell nodules further, aortic allograft paraffin-embedded sections were stained with antibodies to the different Ig heavy-chain isotypes. As in germinal centers, cores of immature double-positive IgM^+ and IgD^+ B cells were surrounded by mature single-positive IgM^+ B lymphocytes (data not shown), and the adventitial B cell aggregates were the site of intense proliferation and apoptosis, as documented by the PCNA staining and the TUNEL assay, respectively (Fig. 4).

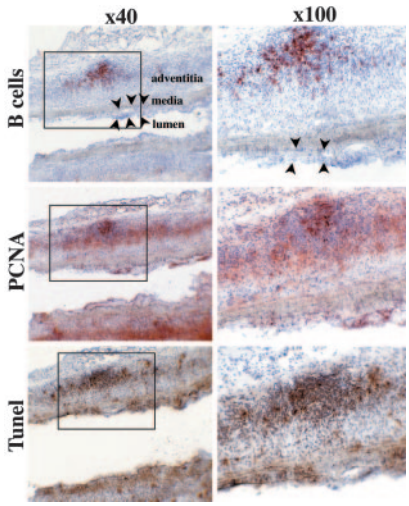

Fig. 4. B cell aggregates in the adventitia are germinal-center-like structures. Immunohistochemistry (alkaline phosphatase anti-alkaline phosphatase technique) was applied to serial 7-μm-thick longitudinal sections of aortic allografts harvested 1 month posttransplantation. Original magnifications, $\times$40 (*Left*) and $\times$100 (*Right*). (*Top*) B cell nodules were detected with an anti-pan B lymphocyte mAb. Neointima development (black arrowheads) could be detected. (*Middle*) Cell proliferation was assessed by PCNA immunohistochemistry. (*Bottom*) The *in situ* DNA TUNEL technique was used to detect apoptosis.

Antibodies Produced in the Adventitia Are Directed to Donor MHC I Molecules. Adventitia, draining lymph nodes, and spleen were cultured so as to collect immunoglobulins produced within these tissues. The supernatants of these cultures were tested on Lewis (recipient) fibroblasts, transfected (LEW-F+$A1^n$) or not transfected (LEW-F) with the RT1-$A1^n$ Brown-Norway (donor) MHC I molecules. Reactivity of antibodies against these cells was evaluated by flow cytometry. Antibodies against the donor MHC I molecules (RT1-$A1^n$), i.e., binding to LEW-F+$A1^n$ cells and not to the untransfected control cells, were present in all of the supernatants from allogeneic grafts (Fig. 5*A*). Strikingly, whereas the amounts of adventitial tissue placed in culture were far less abundant than for cultured spleens or draining lymph nodes, adventitial tissue produced as much alloantibodies as did the spleens and significantly more than did draining lymph nodes (Fig. 5 *A* and *B*). Supernatants from the adventitia of thoracic aortas from grafted animals contained no antibodies (data not shown).

Ectopic Germinal Centers Are Present in Chronically Rejected Human Kidney and Heart Grafts. To evaluate the clinical relevance of the previous observations, we studied surgically removed human heart and kidney grafts by histology. Remarkably, germinal-center-like structures were detected in samples from grafts undergoing chronic rejection (Fig. 6) but not in control organs. Indeed, neither kidneys removed for renal cancer nor renal grafts that were removed early and were therefore devoid of chronic rejection lesions displayed ectopic germinal centers (data not shown). In striking contrast, germinal-center-like structures located in the interstitial tissue were detected in all chronically rejected hearts and kidneys (Fig. 6 *A* and *B*). The core of these structures was composed of proliferating $Ki67^+$ cells (Fig. 6*D*) and B cells (Fig. 6*C*) in close proximity with $CD23^+$ follicular dendritic cells (Fig. 6*E*). This core was surrounded by $CD3^+$ T cells (Fig. 6*F*).

Discussion

In this study, we report previously undescribed immunoinflammatory events closely associated with chronic allograft rejection. Our results suggest that interstitial events play a crucial role in the development of chronic rejection. Evidence obtained from

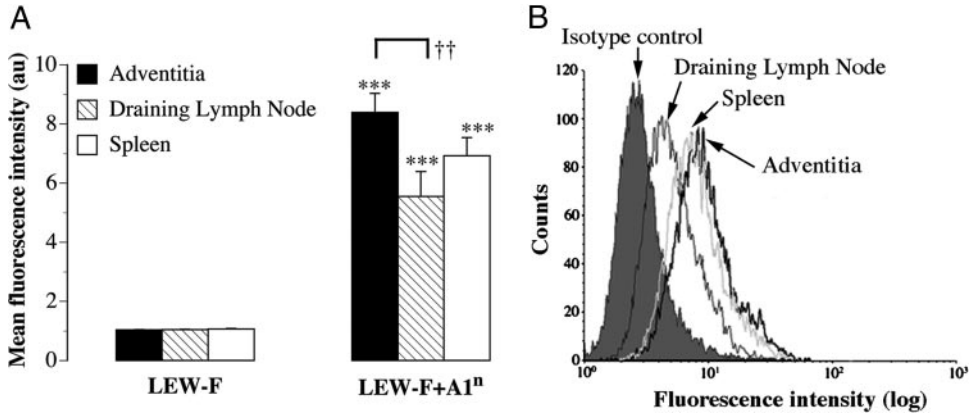

Fig. 5. Antibodies produced in the adventitia are directed to donor MHC I. (*A*) The specificity of the antibodies present in the supernatants from organocultures of adventitia, draining lymph nodes, and spleen was analyzed by flow cytometry using a Lewis (recipient) fibroblast cell line expressing (LEW-F+A1^n) or not expressing (LEW-F) Brown-Norway MHC I molecules. LEW-F and LEW-F+A1^n were incubated with 100 μl of each supernatant. The binding of antibodies on the cell surface was determined with a FITC-conjugated anti-rat Ig κ chain antibody (MARK 1) by measuring the mean fluorescence intensity in a FACScan flow cytometer. ***, $P < 0.0001$ LEW-F vs. LEW-F+A1^n; ††, $P < 0.01$ Adventitia vs. draining lymph nodes. (*B*) A representative histogram overlay is shown.

a rat model of chronic vascular allograft rejection was confirmed on chronically rejected human graft samples.

In the experimental model, we show that (*i*) the number of leukocytes infiltrating the adventitia is related to the amount of allogeneic targets in the graft; (*ii*) the cellular contents of these infiltrates evolves over time and contains mostly CD4$^+$ T helper lymphocytes at 1 month posttransplantation; (*iii*) at 1 month, the adventitial CD4$^+$ T cells express MHC II molecules and CD134, suggesting that they have the capacity to provide help to B cells; (*iv*) B cells infiltrate into the adventitia; (*v*) the adventitial inflammatory infiltrate is organized as a secondary lymphoid tissue, including acquisition by the nearby venular endothelial cells of a HEV-like phenotype; and (*vi*) a humoral alloimmune response against the donor MHC I molecules is elicited within the adventitial ectopic germinal centers. We also show that (*vii*) similar ectopic germinal centers are detected in the interstitial tissue of human heart and kidney chronically rejected grafts. Altogether, these findings suggest that the graft is not only a target for the alloimmune response but is also a site where the humoral alloimmune response is mounted.

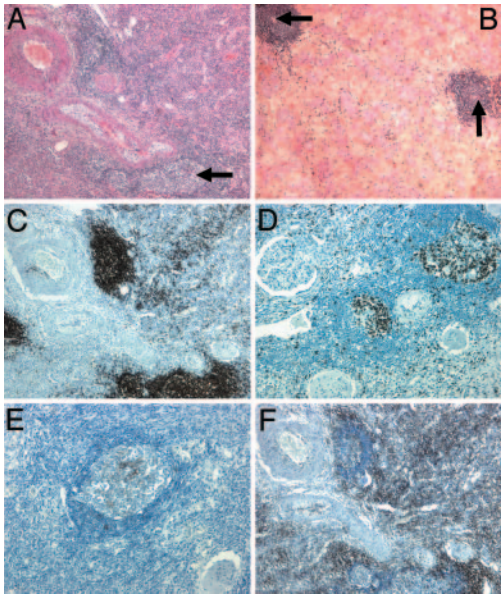

Fig. 6. Ectopic germinal centers are present in human kidney and heart grafts. Human heart and kidney grafts removed because of chronic rejection were studied by histology to determine whether a lymphoid neogenesis process could be detected. Four-micrometer-thick sections of chronically rejected kidney (*A*) and heart (*B*) stained with hematoxylin and eosin displayed germinal-center-like structures in the interstitial tissue nearby a vascular structure (black arrows). Indirect immunohistochemical single staining was performed after a streptavidin–biotin complex method on sections of kidney samples. The following mAbs were used: anti-Ki67 (MiB1, proliferation marker) (*C*); anti-CD20 (L26, anti-pan B cells) (*D*); anti-CD23 (MHM6, anti-follicular dendritic cells) (*E*); and anti-CD3 (polyclonal, anti-pan T cells) (*F*). Original magnifications, ×50 (*A–D*) and ×100 (*E*).

The T cell infiltrate composition at 10 days likely reflects a cytotoxic T cell function, because CD8$^+$ T cells producing IFNγ are abundant. Whereas this initial cellular cytotoxic alloimmune response can rapidly destroy accessible donor endothelial cells, donor smooth-muscle cells, which are protected by elastic lamina, persist in the media 1 month posttransplantation (ref. 17 and data not shown). A previous study has indicated that the immune system uses an alternative strategy to reach the residual allogeneic targets in the media. Indeed, alloantibodies able to cross elastic lamina and induce apoptosis of smooth muscle cells are found in the media (7). Accordingly, we found, at 1 month, that the major part of the T cell infiltrate is composed of CD4$^+$ T cells expressing MHC II molecules, considered to be an activation marker for T cells, and CD134 (OX40), which is expressed on T cells that provide help to B cells (26). Although the phenotype of the T cells present at 1 month posttransplantation in the adventitia suggests that these lymphocytes are involved in the B cell maturation, further studies are required to confirm this hypothesis. An original technical contribution of this work was to set up a tool to quantify the leukocyte infiltrate in the interstitial tissue over time by flow cytometry. Strikingly, and in contrast to previous immunohistological studies (15, 27), this technique allowed us to detect B cells in the adventitial infiltrate of the allograft. The B cells displayed a highly organized nodular disposition that might have prevented their prior detection. Indeed, immunohistological study showed that a ring of single-positive IgM$^+$ B lymphocytes surrounded a core of immature double-positive IgM$^+$ and IgD$^+$ B cells. Our data suggest that these nodules could be ectopic germinal centers.

Because, in most of the inflammatory lesions, the various cells in the infiltrate are not noticeably spatially coordinated, the presence of these highly organized lymphoid structures within the adventitial inflammatory infiltrate was unexpected and raises the question concerning their origin. These germinal centers could arise either from preexisting vascular lymphoid structures or as *de novo* struc-

tures. Wick and coworkers (28) have described a developmentally programmed vascular-associated lymphoid tissue (VALT), which is located in the subendothelial layer of nondiseased arteries. Because the lymphoid structures that we describe are not observed in nondiseased arteries and are exclusively detected in the adventitia, we believe that they are not related to the VALT. Conversely, the adventitial lymphoid architecture that we report could be similar to germinal-center-like organizations originating from the inflammatory infiltrate as *de novo* structures in nonlymphoid tissues. This process, known as lymphoid neogenesis (29), has been described in various tissues subjected to chronic autoimmune aggressions (30, 31) or microbial infections (32). We report here lymphoid neogenesis in alloimmunity.

Germinal centers are generally regarded as specific of developmentally programmed secondary lymphoid organs (lymph nodes, Peyer's patches, and spleen). Because, in these compartmentalized structures, antigen-driven maturation and T cell-dependent activation of naïve B lymphocytes takes place, our observations suggest that naïve alloimmune B cells could be educated within the graft. This hypothesis raises new perspectives regarding the sites able to sustain the initiation of the adaptive immune response to a solid organ allograft. Since the late 1960s, the "peripheral sensitization" concept ascribes to the donor endothelial cells lining vascularized grafts the capacity to activate the allospecific naïve T cells (33). Our study suggests that, in addition to the cell-mediated alloimmune response, the humoral reaction can also be initiated within the graft.

The aggregation of additional observations provides further evidence that the B cell nodules are ectopic germinal centers. First, the B cell nodules observed in the adventitia of allografted aortas were the site of intense proliferation and apoptosis, in accordance with the intensive cell turnover of germinal centers where B cells undergo proliferative rounds and apoptosis associated with somatic hypermutation of their B cell receptor. Second, the spatial compartmentalization of IgM^+ and the IgM^+IgD^+ B cells is the same as in germinal centers. Third, adventitial $CD4^+$ T cells expressed CD134 (OX40). Interestingly, $CD134^+$ cells are found in the T cell zone of lymphoid organs after priming with antigen and the OX40–OX40L interaction is necessary for the *in vivo* differentiation of activated B cells into highly Ig-producing cells (34). Finally, we show that adventitial venular endothelial cells, located within the lymphoid infiltrates, acquired a HEV-like phenotype. HEVs are postcapillary venules specialized in lymphocyte trafficking and are characteristic of lymphoid organs (35). This finding is in accordance with the observation that peritubular capillary endothelium acquires HEV-like properties during acute renal allograft rejection (36). Next, we speculated that the capacity to acquire secondary lymphoid structures, in which B cells would undergo antigen-driven maturation, could be a general feature of interstitial tissue of chronically rejected organs. Interestingly, lymphoid structures have been recently described in murine cardiac allografts undergoing chronic rejection (37). In our study, we extend this finding to human transplantation. Indeed, germinal centers were systematically found in the interstitium of chronically rejected human kidney and heart grafts.

To provide evidence for functional significance of these lymphoid structures in chronic rejection, we had to obtain antibodies produced locally. This technical hurdle was overcome by performing hyperoxic organocultures of adventitia, lymph nodes, and spleen. We demonstrate that the adventitia from aortic graft (but not from the untouched thoracic aorta of the same rat) produces antibodies and that these antibodies are specific for donor MHC I molecules.

In conclusion, the interstitial immunoinflammatory infiltrate organizes itself like a secondary lymphoid structure during chronic rejection. In these local germinal centers, alloantibodies responsible for graft injury are produced. The mechanisms responsible for triggering this lymphoid neogenesis remain to be elucidated. It could result either from a program intrinsic to the local tissue that would be instigated by the chronic inflammation or a general behavior of the immune system that would improve its efficiency by reducing the distance between the effectors and the targets while locally restricting the response. The price to pay for such a local strategy might be that its inadequate control maintains a deleterious ongoing local inflammation. At any rate, the lymphoid neogenesis might be considered as a new therapeutic target in chronic rejection.

We thank Pr. Henri Kreis, Dr. Srini Kaveri, and Dr. Giuseppina Caligiuri for critical reading of the manuscript. U681 is supported by the Institut National de la Santé et de la Recherche Médicale (INSERM) and the Fondation pour la Recherche Médicale; U698 is supported by INSERM and The Leducq Foundation for Cardiovascular Research.

1. Hayry, P., Isoniemi, H., Yilmaz, S., Mennander, A., Lemstrom, K., Raisanen-Sokolowski, A., Koskinen, P., Ustinov, J., Lautenschlager, I. & Taskinen, E. (1993) *Immunol. Rev.* **134,** 33–81.
2. Vongwiwatana, A., Tasanarong, A., Hidalgo, L. G. & Halloran, P. F. (2003) *Immunol. Rev.* **196,** 197–218.
3. Russell, P. S., Chase, C. M. & Colvin, R. B. (1997) *Transplantation* **64,** 1531–1536.
4. Orosz, C. G. (2000) *J. Heart Lung Transplant.* **19,** 634–637.
5. Jin, Y. P., Jindra, P. T., Gong, K. W., Lepin, E. J. & Reed, E. F. (2005) *Transplantation* **79,** S19–S21.
6. Bian, H. & Reed, E. F. (1999) *J. Immunol.* **163,** 1010–1018.
7. Plissonnier, D., Henaff, M., Poncet, P., Paris, E., Tron, F., Thuillez, C. & Michel, J. B. (2000) *Transplantation* **69,** 2601–2608.
8. Lee, R. S., Yamada, K., Houser, S. L., Womer, K. L., Maloney, M. E., Rose, H. S., Sayegh, M. H. & Madsen, J. C. (2001) *Proc. Natl. Acad. Sci. USA* **98,** 3276–3281.
9. Billingham, M. E. (1994) *Clin. Transplant.* **8,** 289–292.
10. Paul, L. C. & Fellstrom, B. (1992) *Transplantation* **53,** 1169–1179.
11. Tilney, N. L., Whitley, W. D., Diamond, J. R., Kupiec-Weglinski, J. W. & Adams, D. H. (1991) *Transplantation* **52,** 389–398.
12. Azuma, H. & Tilney, N. L. (1994) *Curr. Opin. Immunol.* **6,** 770–776.
13. Isik, F. F., McDonald, T. O., Ferguson, M., Yamanaka, E. & Gordon, D. (1992) *Am. J. Pathol.* **141,** 1139–1149.
14. Mennander, A., Tiisala, S., Halttunen, J., Yilmaz, S., Paavonen, T. & Hayry, P. (1991) *Arterioscler. Thromb.* **11,** 671–680.
15. Plissonnier, D., Levy, B. I., Salzmann, J. L., Nochy, D., Watelet, J. & Michel, J. B. (1991) *Arterioscler. Thromb.* **11,** 1690–1699.
16. Schmitz-Rixen, T., Megerman, J., Colvin, R. B., Williams, A. M. & Abbott, W. M. (1988) *J. Vasc. Surg.* **7,** 82–92.
17. Plissonnier, D., Nochy, D., Poncet, P., Mandet, C., Hinglais, N., Bariety, J. & Michel, J. B. (1995) *Transplantation* **60,** 414–424.
18. Battle, T., Arnal, J. F., Challah, M. & Michel, J. B. (1994) *Tissue Cell* **26,** 943–955.
19. Negoescu, A., Lorimier, P., Labat-Moleur, F., Drouet, C., Robert, C., Guillermet, C., Brambilla, C. & Brambilla, E. (1996) *J. Histochem. Cytochem.* **44,** 959–968.
20. Takasaki, Y., Deng, J. S. & Tan, E. M. (1981) *J. Exp. Med.* **154,** 1899–1909.
21. Joly, E., Mucke, L. & Oldstone, M. B. (1991) *Science* **253,** 1283–1285.
22. González-Muñoz, A. L. (1999) Ph.D. thesis (University of Cambridge, Cambridge, U.K.).
23. Gonzalez, A. L., Ruffell, D., Butcher, G. W. & Joly, E. (1995) *Transplant. Proc.* **27,** 1516–1518.
24. van der Loos, C. M., Das, P. K. & Houthoff, H. J. (1987) *J. Histochem. Cytochem.* **35,** 1199–1204.
25. Cattoretti, G., Pileri, S., Parravicini, C., Becker, M. H., Poggi, S., Bifulco, C., Key, G., D'Amato, L., Sabattini, E. & Feudale, E. (1993) *J. Pathol.* **171,** 83–98.
26. Walker, L. S., Gulbranson-Judge, A., Flynn, S., Brocker, T. & Lane, P. J. (2000) *Immunol. Today* **21,** 333–337.
27. Rossmann, P., Lacha, J. & Lodererova, A. (1999) *Folia Microbiol. (Prague)* **44,** 339–353.
28. Waltner-Romen, M., Falkensammer, G., Rabl, W. & Wick, G. (1998) *J. Histochem. Cytochem.* **46,** 1347–1350.
29. Kratz, A., Campos-Neto, A., Hanson, M. S. & Ruddle, N. H. (1996) *J. Exp. Med.* **183,** 1461–1472.
30. Takemura, S., Klimiuk, P. A., Braun, A., Goronzy, J. J. & Weyand, C. M. (2001) *J. Immunol.* **167,** 4710–4718.
31. Salomonsson, S., Jonsson, M. V., Skarstein, K., Brokstad, K. A., Hjelmstrom, P., Wahren-Herlenius, M. & Jonsson, R. (2003) *Arthritis Rheum.* **48,** 3187–3201.
32. Shomer, N. H., Fox, J. G., Juedes, A. E. & Ruddle, N. H. (2003) *Infect. Immun.* **71,** 3572–3577.
33. Lakkis, F. G. (2003) *Am. J. Transplant.* **3,** 241–242.
34. Stuber, E. & Strober, W. (1996) *J. Exp. Med.* **183,** 979–989.
35. Gowans, J. L. & Knight, E. J. (1964) *Proc. R. Soc. London B* **159,** 257–282.
36. Renkonen, R., Turunen, J. P., Rapola, J. & Hayry, P. (1990) *Am. J. Pathol.* **137,** 643–651.
37. Baddoura, F. K., Nasr, I. W., Wrobel, B., Li, Q., Ruddle, N. H. & Lakkis, F. G. (2005) *Am. J. Transplant.* **5,** 510–516.